

The stars near the centre of supergiant shell LMC 4: Further constraints on triggering scenarios*

Jochen M. Braun, Klaas S. de Boer, and Martin Altmann

Sternwarte der Universität Bonn, Auf dem Hügel 71, D-53121 Bonn, Germany
WWW-URL: <http://www.astro.uni-bonn/~webstw>

Received June, 2000; accepted Month, Year

Abstract. The huge supergiant shell (SGS) LMC4, next to the giant HII region 30 Doradus the second most impressive feature of the Large Magellanic Cloud (LMC), has been the subject of many studies and was used to test various models of star forming mechanisms.

In this paper we present a B, V photometry of the very centre of this SGS. The new data yield an age of 11 (2) Myr and a $B - V$ excess of 0.10 (3) mag. Additionally, the two clusters near the geometric centre are too old to be related to the formation of LMC4: HS 343 being ~ 0.1 Gyr and KMHK 1000 being ~ 0.3 Gyr of age. This and existing photometries support that the young stellar population covering the entire inner region is nearly coeval.

We compare these findings with predictions of models proposed for the creation mechanism of SGSs. We conclude that the large-scale trigger, necessary to explain the observations, comes from hydrodynamic interaction of the galactic halo with gas in the leading edge of the moving LMC.

Key words: Stars: early-type – Hertzsprung-Russell (HR) diagram – Stars: formation – ISM: bubbles – ISM: individual objects: LMC4 – Magellanic Clouds

1. Introduction

The creation mechanism for interstellar shells of diameters larger than 300 pc continues to be debated. Such sizes rule out that a single (central) stellar association can provide the energy (the combined effect of SN explosions, stellar winds and radiation pressure) to create such a supershell (see Tenorio-Tagle & Bodenheimer 1988 for a review). Apparently much more energy is needed so that different formation mechanisms have been considered.

In the Large Magellanic Cloud (LMC) Meaburn and collaborators (see e.g. Meaburn 1980) have identified nine supergiant shells (SGSs) based on their filamentary ring-like structure on $H\alpha$ plates. These SGSs have diameters in the range of

0.6 – 1.4 kpc. The largest and best studied is LMC4, which appears in the light of $H\alpha$ as an ellipse of 1 kpc (in E-W) and 1.4 kpc diameter (in N-S direction). In HI it is a thick shell with a gas depleted central area (see, e.g., Luks & Rohlfs 1992; Kim et al. 1999).

The inner part of LMC4 is dominated by the stellar super-association LH77. In literature one finds the name Shapley Constellation III, which is also used for the entire inner part of this SGS. Recently Efremov & Elmegreen (1998) pointed out that this term was used for the wrong object. Originally McKibben Nail & Shapley (1953) ‘defined’ it to be a triple aggregation of $26' \times 26'$ area and to contain NGC 1974. So this name would not be appropriate for the LH77 region (see Fig. 7), but for the N51 region, containing LH63, LH60, and LH54. Thus we consider it best to avoid the ambiguous term Sh III and to only use appropriate object names based on a clear naming convention, like LH nn (Lucke & Hodge 1970; Lucke 1972), N nn (Henize 1956), or LMC4 (Goudis & Meaburn 1978).

Since the identification of LMC4 as SGS, several photometric investigations have been carried out. These aimed, in part, at finding the age of the stars inside LMC4 and at its rim with the goal of tracing the history of the SGS. These studies include those of Isserstedt (1984) and Reid et al. (1987), which indicated propagating star formation, and the recent CCD photometries of Braun et al. (1997) and Dolphin & Hunter (1998), showing a nearly coeval population without any age gradient (see Sect. 3). By now, the CCD studies, in combination with new data presented in Sect. 2, cover about half of the area inside the $H\alpha$ rim. All these studies of the interior agree on the young age of the stars, being of the order of 11-13 Myr, with very little spread. Of course, a much older background population is present, too. But it must be the young stars which are related with the formation of the SGS LMC4.

Additional studies of star groups near the outer edge include those about NGC 1948 (Vallenari et al. 1993; Will et al. 1996), LH63, LH60, LH54 (Petr et al. 1994), LH76 (Wilcots et al. 1996), LH95, LH91 (Gouliermis et al. 2000), NGC 2030 (Laval et al. 1986), and the association LH72 (Olsen et al. 1997) in the (2D projected) central region. The surprising result of these studies is, that the stars *in* the SGS (those near the $H\alpha$ emission) have an age only marginally younger than those in the interior.

Send offprint requests to: jb Braun@astro.uni-bonn.de

* Based on observations collected at the European Southern Observatory (ESO), La Silla, Chile.

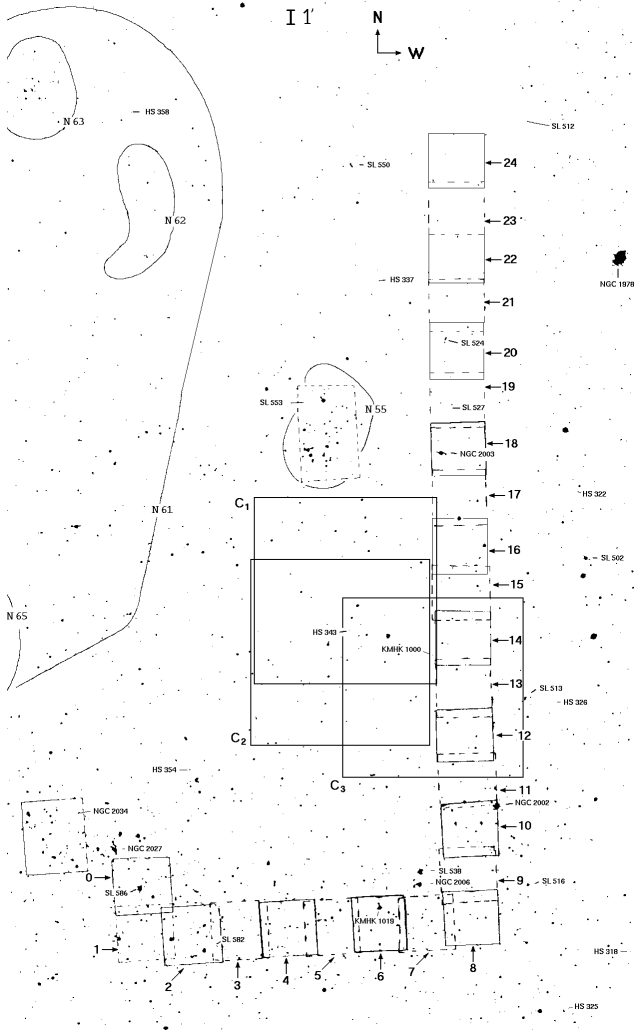


Fig. 1. Mosaic of the central region of LMC4 out of four V charts (44, 45, 51, 52) of the LMC atlas of Hodge & Wright (1967). The 25 fields of the 'J'-shaped area (Braun et al. 1997) and the 3 centre fields C_{1-3} (see Sect. 2) are outlined

The small difference in age between the interior and the edge of LMC4 makes it likely that the stars near the $H\alpha$ emission were formed as a result of the events taking place inside the SGS. However, the sheer volume of space interior to LMC4 containing stars of the same age makes LMC4 a truly exceptional area.

In the present study we have compiled the data and the results on ages and population structure for the LMC4 area. We also add some new photometry, consisting of three fields near the centre covering a total of $167.3 \square'$.

The overall data are analysed to find further clues to the origin of the SGS LMC4. Various mechanisms have been proposed for the formation of LMC4. These include the collision with a high-velocity H I cloud (HVC), the stochastic self-propagating star formation (SSPSF), the triggering of star cluster arcs, and the LMC bow-shock as star formation trigger. These will be discussed, including remarks about their viability and verifiability.

Table 1. Mean DAOPHOT errors and standard deviations of stellar V magnitudes and $B - V$ colours and number of stars in a given magnitude range

Range [mag]	Number of stars	$\overline{\Delta V}$ [mag]	$\overline{\Delta(B - V)}$ [mag]
$V < 18$	2240	0.019 (15)	0.031 (22)
$18 \leq V < 20$	11224	0.025 (16)	0.041 (26)
$20 \leq V$	33285	0.071 (51)	0.127 (90)

2. Observations and data reduction

The new data¹ were taken in January, 1999 with the 1.54 m Danish Telescope at ESO observatory on Cerro La Silla. The telescope was equipped with DFOSC and the $2k^2 \text{ pix}^2$ LORAL CCD (W7 Chip) resulting in a scale factor of $0.39'' \text{ pix}^{-1}$. The chip possesses one 6-fold, six double and six single bad columns plus a 5-fold bad line produced by the electronics on two object frames. Additionally, there were some flatfield problems causing a residual large-scale gradient of up to 4% in V sky flats, so flatfields had to be derived by combining object frames and twilight flats.

The data reduction was performed on GNU/Linux (i386) workstations with MIDAS (see e.g. Banse et al. 1983), IRAF (Tody 1986) and DAOPHOT II (Stetson 1987).

The calibration was achieved using the standard fields SA95 - 42, Rubin 149, PG 1047 + 003, and PG 0918 + 029 (Landolt 1992), observed in B, V passbands at different airmasses on 14th January 1999, yielding an atmospheric extinction of $k_V = 0.163 (32) \text{ mag}$ and $k_B = 0.297 (42) \text{ mag}$ and the calibration constants of Eqs. (1) and (2). After normalization (indicated by the index 'n') to airmass 0 and 1 s exposure time including the PSF to aperture shift ($\delta_V = -0.066 (15) \text{ mag}$ and $\delta_B = -0.005 (20) \text{ mag}$), the following relations were applied:

$$(B - V) = [(B - V)_n - 0.261 (46) \text{ mag}] / 0.931 (18) \quad (1)$$

$$V = V_n - 0.683 (15) \text{ mag} + 0.021 (6) \cdot (B - V) \quad (2)$$

The dataset contains the three fields C_{1-3} of $167.3 \square'$ area (see Fig. 1 for their location and Fig. 3a for an image composit). Each was observed in B, V passbands with short (30 and 15 s) and long (480 and 240 s, respectively) exposures (for field C_3 the exposure times were 240 and 480 s) during a typical seeing of $1.5''$. The entire CCD mosaic shown in Fig. 3a covers $328.5 \square'$.

The brightest star located near the centre of the analyzed area is the galactic F8 dwarf HD 37195 (\equiv P 1313 \equiv MACS J0532-666#013, see Table 3, #7). The compact

¹ The entire Table 4 of this publication is only available electronically, at the CDS (see Editorial in A&A 280, E1, 1993) or at the Astronomical Institutes of Bonn University ('ftp ftp.astro.uni-bonn.de'; further information can be obtained at the URL 'http://www.astro.uni-bonn.de/~jbraun/phdt_lmc4c.html').

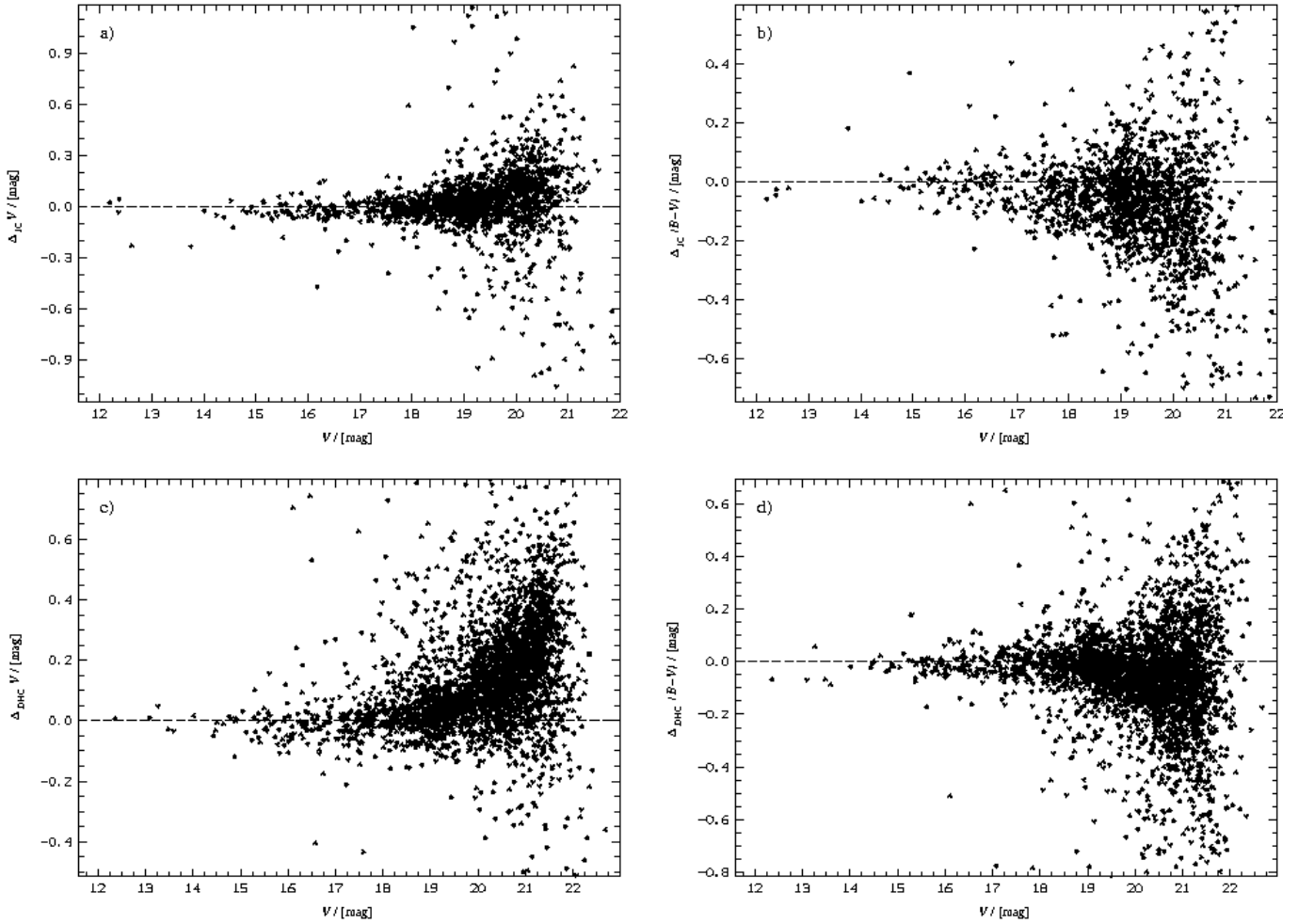


Fig. 2. Photometric comparison of the field C_3 with the overlapping regions of the 'J' dataset (a and b; see Braun et al. 1997) and with the LH77 field (c and d; see Dolphin & Hunter 1998). The zero difference lines are indicated. For details see end of Sect. 2 and Table 2

Table 2. Statistics of the comparison of the three big photometries inside LMC4. The mean (with deviation) of the magnitude and the colour difference is given (compare with Fig. 2)

Fig.	$(\overline{\Delta m})_{br}$ [mag]	N_{br}	$(\overline{\Delta m})_{all}$ [mag]	N_{all}	Range of Δm [mag]
2a	-0.019 (82)	243	0.015 (387)	1739	[-3.71, 5.04]
2b	-0.033 (74)	239	-0.076 (223)	"	[-1.46, 1.78]
2c	0.007 (98)	244	0.140 (219)	3174	[-1.24, 4.43]
2d	-0.008 (57)	239	-0.063 (251)	"	[-4.87, 2.97]

$$2a: \Delta_{JC} V := V_{J,11-15} - V_{C_3}$$

$$2b: \Delta_{JC} (B-V) := (B-V)_{J,11-15} - (B-V)_{C_3}$$

$$2c: \Delta_{DHC} V := V_{DH,LH77} - V_{C_3}$$

$$2d: \Delta_{DHC} (B-V) := (B-V)_{DH,LH77} - (B-V)_{C_3}$$

The brighter subset (indicated by 'br') is defined by

2a and 2c: $V < 18$ mag and $\Delta V \in [-0.6, 0.6]$ mag or

2b and 2d: $V < 18$ mag and $\Delta(B-V) \in [-0.3, 0.25]$ mag

cluster HS 343 = KMHK 1030 (Hodge & Sexton 1966; Kontizas et al. 1990) of ~ 15 pc diameter can be found 2.9 arcmin to the east of star #7 while 2.5 arcmin to the west of star #10

(Table 3 and Fig. 3a) the loose cluster KMHK 1000 of ~ 13 pc diameter is located.

As the western part of the centre field C_3 overlaps with the N-S strip of the 'J'-shaped region (see Fig. 1), Fig. 3 shows both CCD mosaics at the same scale, so e.g. stars marked #9, 13, 15, and 16 on the left panel can easily be found in the right panel.

Table 1 lists photometric errors derived by DAOPHOT and their standard deviation for three magnitude intervals (comparable to the statistical errors given in Table 2 of Braun et al. 1997). The values for the single stars can be found in the resulting data table (Table 4). The quality of all three large photometric studies inside LMC4 can be checked by plotting the magnitude and colour differences of stars in common (see Fig. 2). The mean value, standard deviation, minimum and maximum value of the differences between the photometries of Braun et al. (1997, 'J'), Dolphin & Hunter (1998, 'DH') and the present one ('C') are given in Table 2. Because the data were paired by software, in particular at the faint end mismatches occurred, which affect these values. To determine better statistics, we applied selection criteria given in the footnote of Table 2.

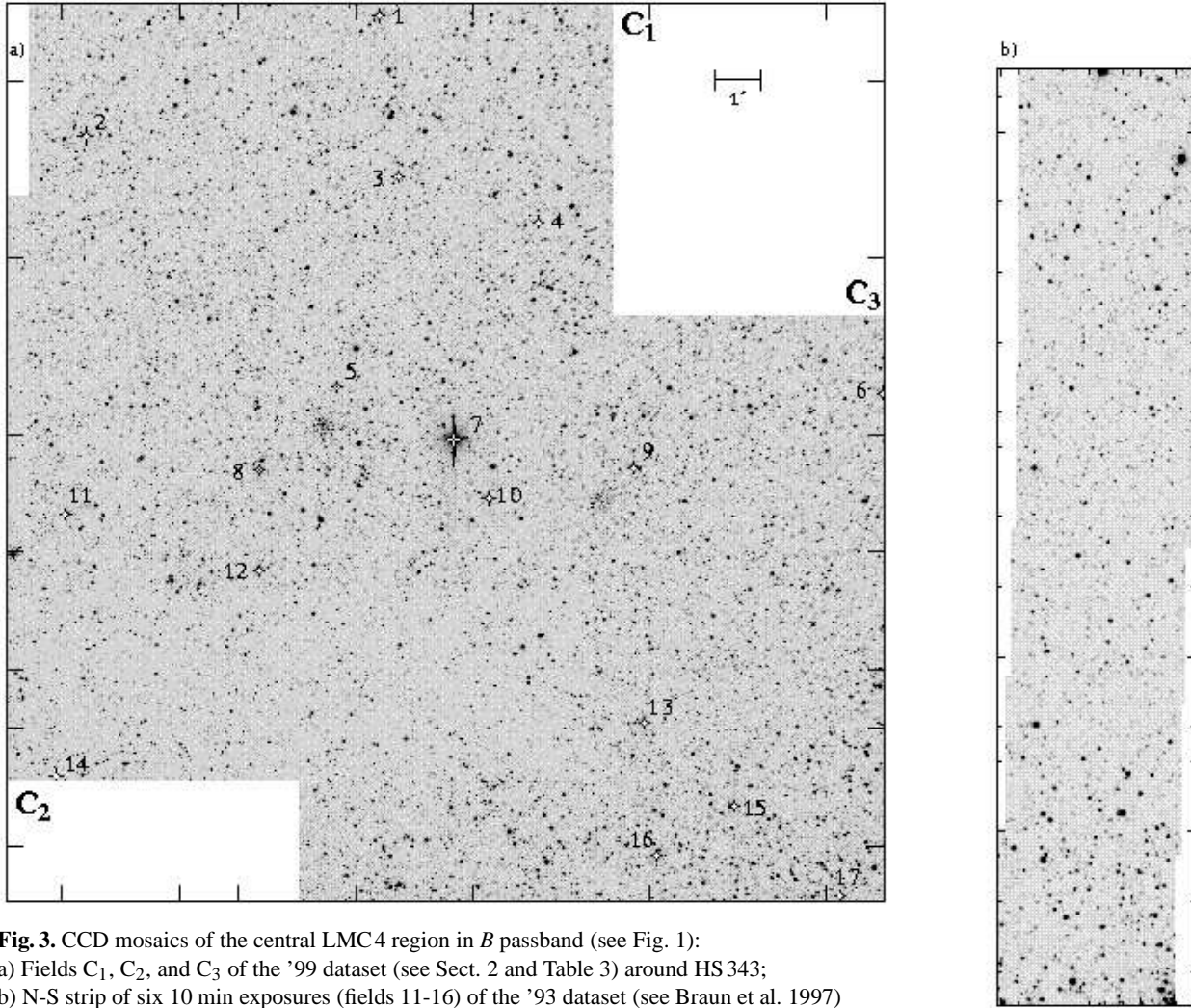


Fig. 3. CCD mosaics of the central LMC4 region in *B* passband (see Fig. 1):

- a) Fields C_1 , C_2 , and C_3 of the '99 dataset (see Sect. 2 and Table 3) around HS 343;
 b) N-S strip of six 10 min exposures (fields 11-16) of the '93 dataset (see Braun et al. 1997)

Table 3. Cross identification of the stars in the central LMC4 area with catalogues by Sanduleak (1969; Sk) or Fehrenbach et al. (1970; P/G), spectroscopic and photometric results compiled by Rousseau et al. (1978; except values in '), IDs in the Magellanic Catalogue of Stars (MACS; Tucholke et al. 1996), and the results of our photometry. The selected stars are labeled in Fig. 3

No. #	Name	Sp LC	<i>V</i> [mag]	<i>B</i> − <i>V</i> [mag]	<i>U</i> − <i>B</i> [mag]	MACS Name	α [^h ^m ^s]	δ [[°] ' ^{''}]	<i>V</i> [mag]	<i>B</i> − <i>V</i> [mag]
1	Sk −66 128	B0 −	12.71	−0.12	−1.01	J0531−665#036	5 31 53.490	−66 31 14.62	12.83	−0.13
2	−	−	−	−	−	J0532−665#041	5 32 59.205	−66 33 49.96	12.49	0.97
3	−	−	−	−	−	J0531−665#033	5 31 49.591	−66 34 49.82	12.28	0.45
4	Sk −66 121	B1 −	13.50	−0.19	−1.05	J0531−665#011	5 31 18.150	−66 35 51.18	13.53	−0.16
5	G 359	A9 I	12.51	0.24	0.23	J0532−666#002	5 32 3.736	−66 39 28.62	12.54	0.19
6	Sk −66 111	B3 I	13.62	−0.17	−0.88	J0530−666#001	5 30 1.331	−66 39 43.56	−	−
7	P 1313	'F8 V'	'9.38'	'0.52'	−	J0531−666#013	5 31 37.185	−66 40 40.57	−	−
8	Sk −66 130	A0 I	12.05	0.04	−0.37	−	5 32 21.212	−66 41 18.65	12.06	0.07
9	Sk −66 120	A0 I	12.50	0.03	−0.31	J0530−666#039	5 30 56.998	−66 41 19.96	12.55	0.04
10	Sk −66 124	A1 I	12.46	0.04	−0.23	J0531−666#012	5 31 29.605	−66 41 59.23	12.48	0.06
11	G 375	B6 I	'13.10'	−	−	J0533−667#004	5 33 4.862	−66 42 14.74	12.98	−0.03
12	Sk −66 129	A0 I	12.16	0.06	−0.19	J0532−667#015	5 32 21.704	−66 43 33.72	12.15	0.07
13	Sk −66 119a	A0 I	12.16	0.07	0.00	J0530−667#030	5 30 55.034	−66 47 1.30	12.19	0.11
14	−	−	−	−	−	J0533−668#006	5 33 7.603	−66 48 5.55	12.50	1.82
15	Sk −66 117	B2 −	12.36	−0.06	−0.76	J0530−668#029	5 30 35.007	−66 48 53.05	12.36	−0.03
16	Sk −66 119	B8 I	12.17	0.16	−0.34	J0530−668#051	5 30 52.181	−66 49 58.49	12.37	0.03
17	−	−	'13.45'	'−0.14'	'−0.93'	J0530−668#010	5 30 10.589	−66 50 54.92	13.47	−0.08

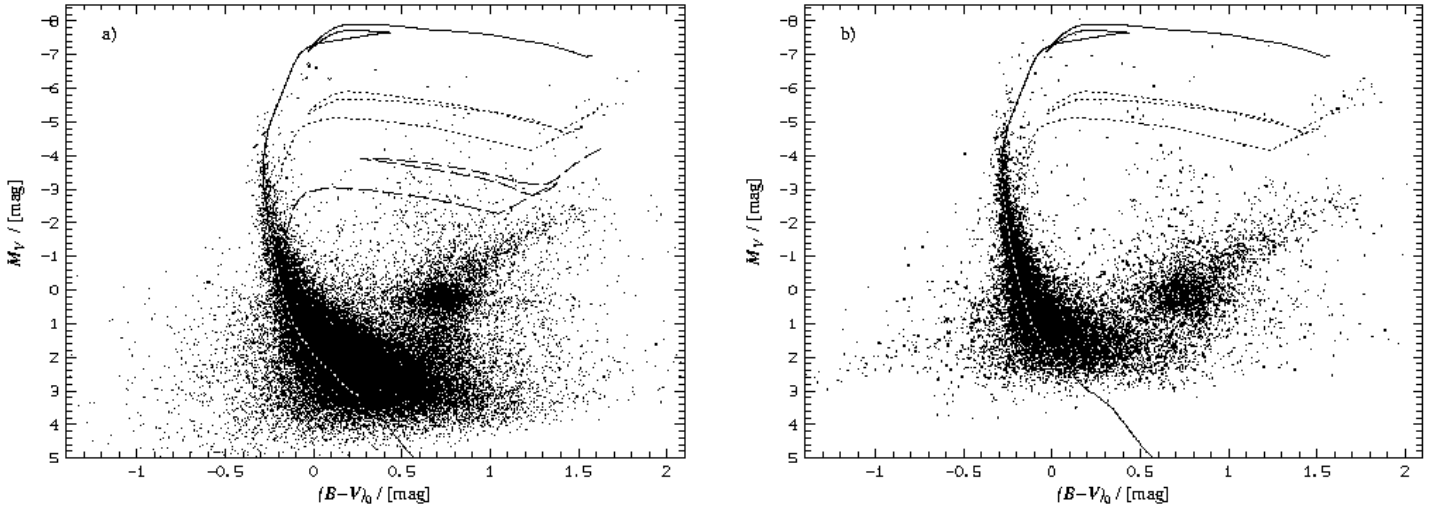


Fig. 4. CMDs of LMC4 with the isochrones of the Geneva group (Schaerer et al. 1993) for LMC metallicity ($Z = 0.008$) and for logarithmic ages $\log(t/[\text{yr}]) \in \{7.05, 7.5, 8.0\}$ and extinction correction of $A_V = 0.31$ mag.

a) CMD with 46749 data points of the LMC4 centre fields C_1 , C_2 , and C_3 [left panel].

b) CMD with 15787 data points of the LMC4 'J' dataset (Braun et al. 1997) without fields 11-16 [right panel].

In panel a) the crosses near $M_V \approx -6.5$ mag are 6 A supergiants (see end of Sect. 3)

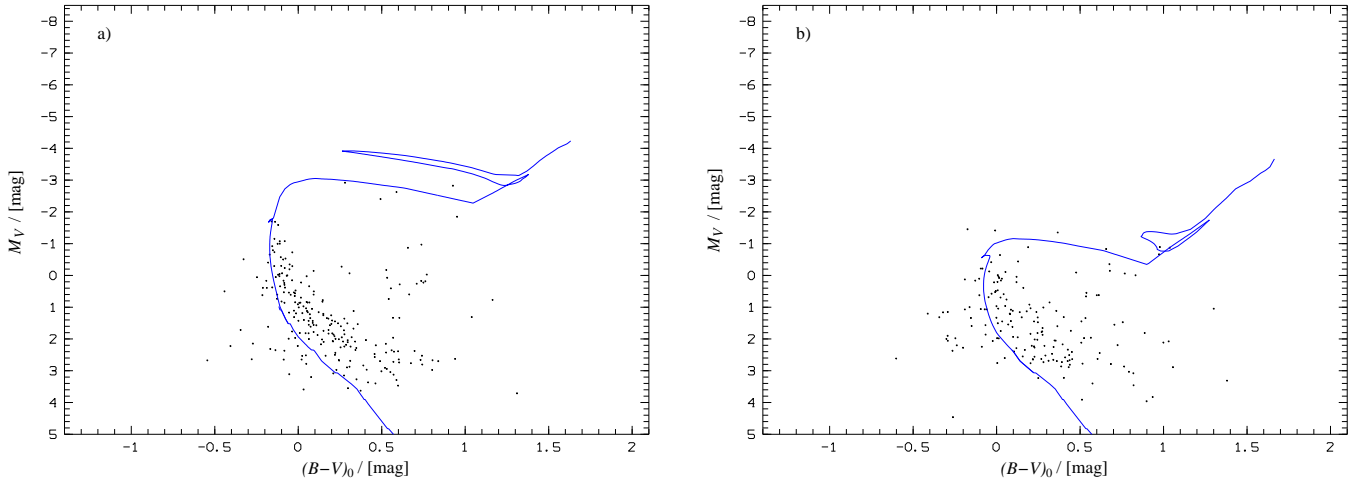


Fig. 5. CMDs of two clusters in the central region of LMC4, i.e., part of the data plotted in Fig. 4a.

a) CMD of the circular region with radius of $34'' = 8.3$ pc around HS 343 containing 237 data points [left panel].

b) CMD of the circular region with radius of $30'' = 7.3$ pc around KMHK 1000 with 175 data points [right panel].

The isochrones of the Geneva group (Schaerer et al. 1993) of 0.1 Gyr and 0.3 Gyr show that these stars are 'old' and are not related in any way with events leading to the existence of supergiant shell LMC4

Table 4. Small part of the resulting photometric data showing five entries around G 359 (see #5 in Table 3). Stars are identified by their field sequence numbers. The coordinates (α, δ) derived from the MACS reference grid are given along with the calibrated V magnitudes, $B - V$ colours and the photometric errors (from DAOPHOT). The entire table with 46749 entries is available electronically, see the footnote to Sect. 2

Field sequ.	α [^h ^m ^s]	δ [[°] ['] ^{''}]	V [mag]	ΔV [mag]	$B - V$ [mag]	$\Delta(B - V)$ [mag]
:	:	:	:	:	:	:
1.010774	5 31 7.233	-66 39 27.97	20.728	0.047	0.818	0.100
1.010460	5 33 8.814	-66 39 27.99	21.046	0.048	0.287	0.068
1.112922	5 32 3.793	-66 39 27.99	12.543	0.013	0.189	0.022
3.026160	5 30 11.500	-66 39 27.99	18.807	0.060	0.026	0.102
3.025976	5 31 20.923	-66 39 28.02	21.388	0.041	0.473	0.187
:	:	:	:	:	:	:

Even though the new dataset covers a larger area ($A_{C_{1-3}} \approx 1.1 \cdot A_J$), the colour-magnitude diagram of the new data (Fig. 4a) shows less upper main sequence stars than the CMD of the earlier data (Fig. 4b). This is caused by the larger stellar density in the E-W portion, i.e. fields 0-9 of the 'J'-shaped region containing a part of LH77. The combined datasets cover $574 \square'$ on the sky, i.e. about 11% of the LMC4 area as defined by the H α filaments.

To calculate absolute magnitudes we used the distance modulus of $(m - M)_0 = 18.5$ mag, which is still the *best* applicable value. Gibson (2000) gives a range of current determinations of [18.07, 18.74] mag (see also Groenewegen & Oudmaijer 2000).

The isochrones of the Geneva group (Schaerer et al. 1993) for LMC metallicity ($Z = 0.008$ or $[\text{Fe}/\text{H}] = -0.34$ dex) had been fitted by eye, yielding age and interstellar extinction as given in the next section.

3. Results of photometric analyses

To determine the age of stellar populations inside LMC4 we had already obtained CCD photometry in B, V passbands (Braun et al. 1997). The two strips with a total of 25 CCD positions (see Fig. 1) cover 298 arcmin² equivalent to 6% of the area inside the H α filaments. This 'J'-shaped area constitutes an E-W strip of 400 pc in the region of the OB superassociation LH77 and a S-N strip of 850 pc.

The colour-magnitude diagrams (CMDs) and luminosity functions (LFs) derived from the data yielded ages of 9 – 16 Myr, a colour excess of mostly only 0.11 mag (in some places even less), and LF slopes of 0.22-0.41 (Braun et al. 1997; Braun 1996). The age range given is maximized but nevertheless by a factor 2 smaller than the necessary age spread required by the global SSPSF scenario (see Sect. 5.2). Additionally, no correlation with the distance to the centre of LMC4 was found. In all CMDs a young population of about 11 Myr is present, even though the stellar density of this population gets low towards the north leading to the higher LF slopes (compared to an expected slope $\gamma = 0.27$, see Will 1996).

Dolphin & Hunter (1998) analyzed UBV photometry of four fields inside LMC4 and one field outside, near its rim. This study yields ages of 12-16 Myr and $B - V$ excess reaching from 0.04 to 0.07 mag inside LMC4 and ~ 7 Myr and 0.09 mag for the NGC 1955 field (i.e. the N51 region). The lack of an age gradient inside the SGS is supported.

These studies can now be extended by the present B, V CCD photometry for three positions of the central region inside SGS LMC4 (see Fig. 1), which are centered near the clusters HS 343 and KMHK 1000. The observed area of 69 500 pc² would contain the stellar population predicted to be 30 Myr of age according to the model of the triggered star cluster arcs (see Sect. 5.3), even if that population were spatially dispersed.

The isochrone fit to the new dataset yields an age of 11 (2) Myr and a colour excess $E_{B-V} = 0.10$ (3) mag. This value was also checked by deriving intrinsic colours and thus reddening by the Wesenheit function (see e.g. Hill et al. 1994): $W := V - 3.1 \cdot (B - V)$ and an appropriate fit to the stellar evo-

Table 5. Age (t) and reddening (E_{B-V}) of star populations inside and at the edge of LMC4 sorted from north to south, see Figs. 1 and 7

Object	t [Myr]	E_{B-V} [mag]	Paper
<i>Inside LMC4:</i>			
'C' region	11	0.10	this paper
'J' region	9-16	$\lesssim 0.11$	Braun et al. 1997
4 inside fields	12-16	0.04-0.07	Dolphin & Hunter 1998
<i>Edge of LMC4:</i>			
NGC 2030	4	0.19	Laval et al. 1986
NGC 1948	5-10	0.20	Will et al. 1996
LH91, 95	~ 8	0.17	Gouliermis et al. 2000
LH72, north	8-15	0.00-0.04	Olsen et al. 1997
LH72, south	5	0.06-0.17	Olsen et al. 1997
NGC 2004	16	0.09	Sagar & Richtler 1991
LH63	14	0.07	Petr 1994
LH60	9	0.04	Petr 1994
NGC 1955	7	0.09	Dolphin & Hunter 1998
LH54	6	0.10	Petr 1994
LH76	2-5	0.09	Wilcots et al. 1996

lution model. We used the main sequence (MS) stars with $V \in [14.7, 17.5]$ mag and an isochrone of $\log(t/[\text{yr}]) = 7.05$ yielding $(B - V)_0 \approx -0.693 \text{ mag} + 0.025 \cdot W$. The E_{B-V} -distribution of these 629 MS stars has its maximum at 0.1 mag with a mean (and deviation) of 0.12 (4) mag.

The similarity of the morphology visible in the CMDs of the two datasets, the one (Fig. 4a, fields C_{1-3}) containing the populations at the LMC4 centre and the other (Fig. 4b, fields 0 – 10 and 17 – 24) being dominated by the superassociation LH77, is striking. No population of age 30 Myr is present in the central part. This follows directly from the comparison of the region in both CMDs to the right of the main sequence, near the 30 Myr isochrone.

The members of the group of six A-type supergiants near HS 343 (see Fig. 6; these stars selected by Efremov & Elmegreen 1998 from the data of Rousseau et al. 1978 are No. 5, 8, 9, 10, 12, and 13 of Table 3), quoted as relicts of a 30 Myr population, are marked by crosses in Fig. 4a. The CMDs for the two clusters near the geometric centre of the filamentary H α boundary show their ages to be ~ 0.1 Gyr for HS 343 and ~ 0.3 Gyr for KMHK 1000 (see Fig. 5).

4. Age structure inside LMC4

The similarity of the morphology visible in the CMDs of all datasets is striking. Therefore the stars inside LMC4 must have been formed in a short period of time, so the H α and H I feature called LMC4 must have been created in a turbulent manner rather than in a 'bubble blowing' action. This fits also to the small (i.e. $\ll 500$ pc) disk thickness of the LMC (e.g. Kim 1998 derived in Sect. 5.2.1 an exponential scale height of the gas of ~ 170 pc, i.e. a disk thickness of ~ 340 pc). This implies that this SGS resembles a truncated cylinder rather than a bubble. The onset of this star burst can be dated by isochrone fitting

giving as average age of the interior population 12 (2) Myr. No other population of age less than 100 Myr is present in the central part.

The star groups near the edge are younger indeed than the stars in the interior of LMC4. The age at the edge (age of stars associated with the H α emission outside the H α rim of the SGS) is 4-7 Myr (see Table 5 and Sect. 6.1). This implies that ~ 5 Myr after the giant central volume formed stars, the edge was pushed into star formation mode, too.

One is thus faced with several questions pertaining to the origin of the structure called LMC4. What mechanism can stimulate *simultaneous* star formation over an area (in a volume) with projected size of about $800 \text{ pc} \times 1200 \text{ pc}$ (the interior of LMC4)? By what mechanism was the gas of the birth cloud dispersed so efficiently to create the presently low column densities in the H I over such an area? What stimulated the star formation at the outskirts of this area (creating the H α structure called LMC4) in a relatively homogeneous manner?

5. Discussion of scenarios proposed for LMC4's creation

Several star formation scenarios possibly leading to the formation of supergiant shells are mentioned in the literature. Here we will comment on each in relation with our knowledge of LMC4.

5.1. HVC infall

An infalling high-velocity cloud might compress the gas in the LMC disk and so trigger star formation.

Infall would affect star formation in a large region indeed and we see that the ages derived for the large inner part of LMC4 are equal (see Sect. 3). However, the data about the density and radial velocity of LMC4 gas contradict this scenario (Domgörgen et al. 1995), and infall was not the actual trigger for the formation of LMC4.

In addition, given the motion of the LMC through the halo of the Milky Way (Kroupa & Bastian 1997), the velocity of such a HVC should have been rather orthogonal to that of the LMC itself, thus having a velocity vector pointing more or less toward the Sun. A HVC moving away from the Milky Way is very unlikely. HVCs moving toward the Milky Way at $+60$ and $+120 \text{ km s}^{-1}$ are known in this direction (Savage & de Boer 1979). Since this high velocity gas is seen over the entire face of the LMC (see Savage & de Boer 1981), with the LMC at $v_{\text{rad}} \approx 250 \text{ km s}^{-1}$, it is rather nearby.

5.2. SSPSF

In the stochastic self-propagating star formation scenario the stars formed initially trigger further star formation in their vicinity.

SSPSF leads to an age gradient from the starting point, e.g. the centre of a SGS, outward to the rim (Feitzinger et al. 1981). It has been a popular model and was often cited in papers about

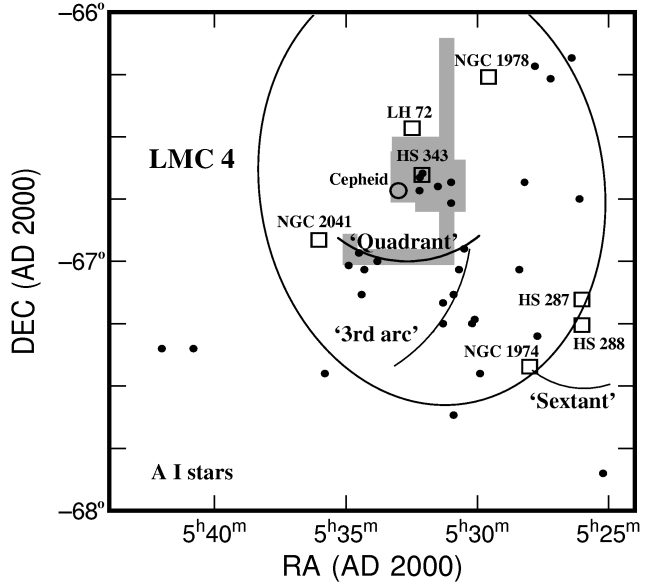


Fig. 6. Schematic plot of selected structures near LMC4. The ellipse shows the location of the H α filaments and the H II regions, the gray area the regions covered by the present and the earlier (Braun et al. 1997) photometry. Some of the structures mentioned by Efremov & Elmegreen (1998) in relation with arc formation (the arcs, some A I stars from Rousseau et al. 1978, the Cepheid HV2667, erroneously given as HV 5924 by Efremov & Elmegreen) are indicated (figure adapted from Fig. 2 of Efremov & Elmegreen 1998)

supershells in distant galaxies where no photometry of individual stars is available.

The predictions by SSPSF for the morphology of SGSs agree with the observed density and radial velocity of gas in the interior of LMC4. However, the large radius of the SGS would lead to a continuous age spread of the stars of at least 15 Myr range. Even if one takes a possible overlap of stellar populations having different ages into account, the photometric data are in contradiction with such a population structure and thus indicate incompatibility of the SSPSF scenario with the interior of LMC4. This has now been sufficiently noted (see Braun et al. 1997; Dolphin & Hunter 1998).

5.3. Triggering of stellar arcs

Star clusters or γ -ray bursts may trigger star formation to form arc like structures.

Efremov & Elmegreen (1998) suggested as trigger for star formation in LMC4 the self-gravitational collapse of parts of rims from shells initially driven by star clusters, leading to the building of star cluster arcs. They identify three of these structures (see Fig. 6), circular (in the 2d projection) in shape, and this may indicate that they have been formed by swept-up material. Efremov et al. (1998) subsequently suggested that gamma-ray bursts (GRBs) may produce the pressurizing wave.

These suggestions are rather *ad hoc*. Moreover, they would create localized structures and nothing of the kind like LMC4. The collapse into a cluster or the explosion of a GRB, formation

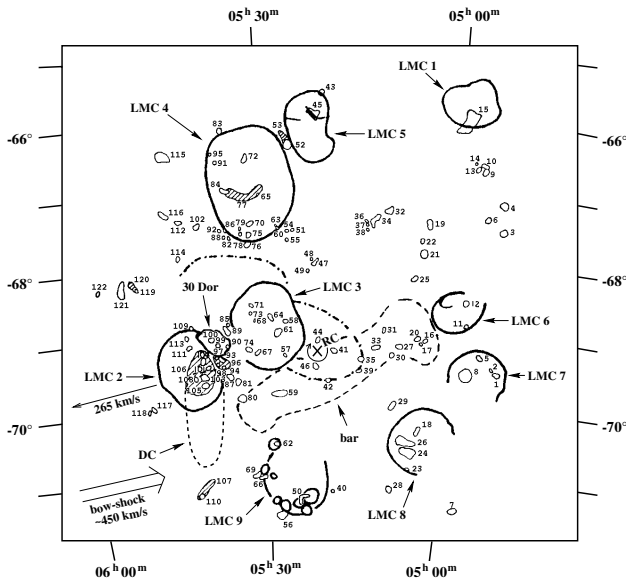


Fig. 7. Sketch of the LMC with the nine supergiant shells (LMC 1 - LMC 9) and the giant HII region 30 Doradus (from Meaburn 1980, Fig. 2), the dark cloud (DC) south of 30 Dor, the 122 OB associations (LH nm , from Lucke & Hodge 1970, Fig. 1), and the isophote of the bar (from Smith et al. 1987, Fig. 4). The LMC has an imprecisely defined rotation centre, situated near RC. The movement of the LMC in the galactic halo is indicated by the direction of the proper motion. The resulting bow-shock, driven by the sum of motion and rotation, is $\sim 450 \text{ km s}^{-1}$ (see de Boer et al. 1998)

of a shell of swept up material which itself forms stars, which then leads to a next shell or the acceleration of the old shell (the scenario for the ‘Quadrant’ and subsequently for LMC4 after Efremov & Elmegreen 1998) may explain some features, but not the entire SGS with the documented age structure (see Sect. 4). Furthermore it is hard to explain why ‘Quadrant’ is coeval (Braun et al. 1997) while ‘Sextant’ shows a clear age gradient (Petr et al. 1994) if the same mechanism would be valid. The geometry of the (after Efremov & Fargion 2000) four cluster arcs are rather due to cloud structure long *before* star formation than being directly connected to the formation process.

5.4. Star formation triggered by the LMC bow-shock

The motion of the LMC through the Milky Way halo leads to a bow-shock triggering star formation.

Since a very large area created stars at the same time, and since (due of the rotation of the LMC) the present day LMC4 was near the leading edge about 15 Myr ago, the bow-shock of the LMC may have triggered the conditions for large-scale star formation. Searching for a possible creation mechanism of supergiant shell LMC4 and maybe of all the supershells of the Large Magellanic Cloud, one finds that the superstructures of the LMC (see Fig. 7) are all located at the outskirts. Looking at these features clockwise from south-east to north-west, the

expected correlation of age with traversed distance is visible (see de Boer et al. 1998).

The scenario has as essential part the motion of the LMC through the galactic halo and the LMCs clockwise rotation. The gas of the LMC rotates through the compression zone at the south-east, to eventually find itself in the north-east (LMC4) with all the consequences of the star formation triggered inside that gas.

6. Summary and conclusions

In the review of the scenarios above we have indicated that the first three are not compatible with the observational facts. The most important fact is that over the entire interior of LMC4 star formation burst out on a large scale about 12 Myr ago (see Table 5 and Sects. 3 and 4). Small stellar associations cannot be used as trigger for large-scale structures and there is no evidence for a recent collision with a HVC. The bow-shock formation scenario is the only viable one. Note that the bow-shock scenario explains only the formation of large structures around the edge of the LMC. At any given location in the LMC star formation continues as is readily visible from the ubiquitous H α structures everywhere in the LMC.

6.1. Evolution after the star burst took place

After formation of the original cloud of stars these stars emitted their energy into the surroundings, driving the gas out of this region rather more in a turbulent than a pressurized manner. The total energy produced by the massive stars, (stellar winds, ionizing photons, and supernova explosions) went into ionizing and expansion of the original birth cloud. These aspects have been discussed by Braun et al. (1997) and by Dolphin & Hunter (1998) and are not repeated here.

After the formation of this 1st generation of stars, star formation was initiated at the edge of the central region, creating populations of younger ages visible by the HII regions surrounding this SGS. Examples for these stellar populations are LH63, LH60 and LH54 (Petr et al. 1994), situated in the N51 region, and LH76 (Wilcots et al. 1996) more to the east (see Fig. 7 and Table 5). Also part of LH72 (Olsen et al. 1997) is one of these, assuming it lies somewhat outside the plane of LMC4, being at a different depth in the LMC. This phase with the formation of stars at the outskirts of the original cloud affects only regions of small size (i.e. $< 300 \text{ pc}$) as expected from the limits due to inhomogeneity (density, temperature, magnetic fields etc.) of the medium.

6.2. Details of the bow-shock formation and consequences for the overall structure of the LMC

The convergence of gas near the bow-shock, due to the LMC space motion combined with the LMCs rotation (see de Boer et al. 1998) creates a large and condensing gas cloud. In it star formation sets in, and the rotation of the LMC moves this region around the edge in clock-wise fashion.

The role of ram-pressure, especially the comparison of strength of hydrodynamic and gravitational effects, is still uncertain. Observational findings like X-ray shadowing (Blondiau et al. 1997), the steep edge in HI near the location of the largest velocity with respect to the halo gas (see e.g. the map by Kim et al. 1999), and H α emission of some main components of the Magellanic Stream (Weiner & Williams 1996) are all indications for bow-shocks due to motion of Magellanic material through halo gas. To fit the HI maps of the Stream and other structures, recent models for the tidal interactions of the Magellanic Clouds (MCs) are extended by a drag term (Gardiner 1999), accounting for the motion of the MCs through the Milky Way halo. However, problems remain and not all inconsistencies are solved (see e.g. Moore & Davis 1994 and Murali 2000).

The shape of the dark cloud presently seen south of 30 Dor is elongated, oriented perpendicular to the direction of the rotation centre of the LMC. The most dense region of stars inside LMC4, being the hatched region in Fig. 7 with the embedded smaller associations LH65 and LH84, has the same orientation. We note that at their radial distance from the centre (both at approximately 2 kpc) the LMC rotation curve is rather level, and rotation will hardly change the original shape of structures.

Since the density of the LMC drops radially outward, it is to be expected that older SGSs will have opened up to the LMC edge. The morphology of the H α distribution may therefore give further evidence for the expected age sequence of the SGSs. Continuing in clockwise direction, the supergiant shell LMC5 to the east of LMC4 is still complete, while LMC6 is a non-contiguous ring. Note also, that the star density in LMC4 drops outward and that LMC4 is elongated toward the lower density on the outside.

Apart from the young stars in LMC4 older populations are present. These may date from a previous burst, of one or more revolutions ago. Such earlier events will have left numerous earlier generations. However, a bow-shock triggered burst need not take place continuously, since apparently gas accumulates intermittently and the power of the trigger is sensitive to the current halo density at the front of the LMC. If it were continuous, one would see a continuous ring of young stars around the LMC's edge.

The age of small-scale structures may or may not be related to the age of the large-scale structures such as LMC4. One full rotation of the LMC edge takes $\simeq 100$ Myr so that larger older structures may be part and/or consequence of a previous large-scale event.

6.3. Comparison with other dwarf galaxies

Looking at other dwarf galaxies in H α or HI, one recognizes that supershells are quite common features in galaxies and especially in dwarf galaxies (e.g. Brinks & Walter 1998), where the symmetry is not disturbed by differential rotation. However the different environment of these galaxies, such as tidal forces from neighbouring galaxies or being completely isolated, makes it difficult to explain these supershells by the same

creation mechanism as the supergiant shells in the Magellanic Clouds. Still, in such galaxies larger volumes of space must attract sufficient amounts of gas in dense form that a starburst takes place, setting off star formation nearly simultaneous in huge volumes.

Clearly, photometric studies of resolved stellar populations in more distant (dwarf) galaxies are needed to achieve a general picture on these large-scale star forming processes.

6.4. Conclusions

The photometry of large areas inside LMC4 shows that the stars are of the same age, being $\simeq 12$ Myr. The rotation speed of the LMC makes clear that the LMC4 region was at time 0 near the bow-shock. At the bow-shock one currently finds a huge dark cloud being in the process of forming stars. Combining these two observational facts led to the bow-shock scenario and further evidence has been brought forward to substantiate this scenario.

Observing the interior of further supergiant shells will provide clearer insight in the formation history of the star groups inside such structures. Except for the complicated 30Dor region (with the neighbouring supergiant shells LMC2 and LMC3) all other SGSs should show a coeval large-scale stellar population fitting to the age sequence proposed by the bow-shock scenario. Were this found to be not so, then the bow-shock trigger model would be falsified. One then would be in need of finding another star formation trigger. Given the current observations the only other possible (however unlikely) scenario would then be a special HVC collision. As yet, the bow-shock induced star formation fits the available observational data best.

Acknowledgments

JMB was partly supported through the Deutsche Forschungsgemeinschaft (DFG) in the *Graduiertenkolleg* 'The Magellanic Clouds and other Dwarf Galaxies', MA by the DFG through grant Bo 779/21.

We wish to thank Dr. Deidre A. Hunter for providing us a CCD image of their LH77 field for star identification.

References

- Banse K., Crane P., Grosbøl P., et al., 1983, ESO Messenger 31, 26
- Blondiau M.J., Kerp J., Mebold U., Klein U., 1997, A&A 323, 585
- Braun J.M., 1996, Diploma Thesis, University of Bonn
- Braun J.M., Bomans D.J., Will J.-M., de Boer K.S., 1997, A&A 328, 167 (arXiv:astro-ph/9708081)
- Brinks E., Walter F., 1998, in 'The Magellanic Clouds and Other Dwarf Galaxies', Workshop Proceedings of the Bonn/Bochum-Graduiertenkolleg, Richtler T., Braun J.M. (eds.), Shaker Verlag, Aachen, p. 1 (electronic version available at the URL: 'http://www.astro.uni-bonn.de/~webstw/brinks_r.html', see index at arXiv:astro-ph/9811445)
- de Boer K.S., Braun J.M., Vallenari A., Mebold U., 1998, A&A 329, L49 (arXiv:astro-ph/9711052)

- Dolphin A.E., Hunter D.A., 1998, *AJ* 116, 1275
- Domgörgen H., Bomans D.J., de Boer K.S., 1995, *A&A* 296, 523
- Efremov Y.N., Elmegreen B.G., 1998, *MNRAS* 299, 643
(arXiv:astro-ph/9805092)
- Efremov Y.N., Fargion D., 2000, *A&A* in press
(arXiv:astro-ph/9912562)
- Efremov Y.N., Elmegreen B.G., Hodge P.W., 1998, *ApJ* 501, L163
(arXiv:astro-ph/9805236)
- Fehrenbach Ch., Duffot M., Petit M., 1970, *A&A Special Supl.* 1, 1
- Feitzinger J.V., Glassgold A.E., Gerola H., Seiden P.E., 1981, *A&A* 98, 371
- Gardiner L.T., 1999, in ‘High Velocity Clouds’, Stromlo Workshop, Gibson B.K., Putman M.E. (eds.), ASP Conf. Ser. 166, 292
- Gibson B.K., 2000, *Mem. Soc. Astron. Italiana*, in press
(arXiv:astro-ph/9910574v2)
- Goudis C., Meaburn J., 1978, *A&A* 68, 189
- Gouliermis D., de Boer K.S., Keller S.C., Kontizas M., Kontizas E., 2000, in prep.
- Groenewegen M.A.T., Oudmaijer R.D., 2000, *A&A* 356, 849
(arXiv:astro-ph/0002325)
- Henize K.G., 1956, *ApJS* 2, 315
- Hill R.J., Madore B.F., Freedman W.L., 1994, *ApJ* 429, 192
- Hodge P.W., Sexton J.A., 1966, *AJ* 71, 363
- Hodge P.W., Wright F.W., 1967, *The Large Magellanic Cloud*, Smithsonian Press
- Isserstedt J., 1984, *A&A* 131, 347
- Kim S., 1998, Ph.D. Thesis, Australian National University
- Kim S., Dopita M.A., Staveley-Smith L., Bessell M.S., 1999, *AJ* 118, 2797
- Kontizas M., Morgan D.H., Hatzidimitriou D., Kontizas E., 1990, *A&AS* 84, 527
- Kroupa P., Bastian U., 1997, *New Astr.* 2, 77
- Landolt A.U., 1992, *AJ* 104, 340
- Laval A., Greve A., van Genderen A.M., 1986, *A&A* 164, 26
- Lucke P.B., 1972, Ph.D. Thesis, University of Washington
- Lucke P.B., Hodge P.W., 1970, *AJ* 75, 171
- Luks Th., Rohlf K., 1992, *A&A* 263, 41
- McKibben Nail V., Shapley H., 1953, *Proc. Nat. Acad. Sci.* 39, 358
- Meaburn J., 1980, *MNRAS* 192, 365
- Moore B., Davis M., 1994, *MNRAS* 270, 209
(arXiv:astro-ph/9401008)
- Murali C., 2000, *ApJ* 529, L81 (arXiv:astro-ph/9912168)
- Olsen K.A.G., Hodge P.W., Wilcots E.M., Pastwick L., 1997, *ApJ* 475, 545
- Petr M., 1994, Diploma Thesis, University of Bonn
- Petr M., Bomans D.J., Grebel E.K., 1994, in 3rd CTIO/ESO Workshop on the Local Group Layden A., Smith R. C., Storm J. (eds.), ESO Conf. Proc. 51, 86
- Reid N., Mould J., Thompson I., 1987, *ApJ* 323, 433
- Rousseau J., Martin N., Prévot L., et al., 1978, *A&AS* 31, 243
- Sagar R., Richtler T., 1991, *A&A* 250, 324
- Sanduleak N., 1969, CTIO, Contribution No. 89
- Savage B.D., de Boer K.S., 1979, *ApJ* 230, L77
- Savage B.D., de Boer K.S., 1981, *ApJ* 243, 460
- Schaerer D., Meynet G., Maeder A., Schaller G., 1993, *A&AS* 98, 523
- Smith A.M., Cornett R.H., Hill R.S., 1987, *ApJ* 320, 609
- Stetson P.B., 1987, *PASP* 99, 191
- Tenorio-Tagle G., Bodenheimer P., 1988, *ARA&A* 26, 145
- Tody D., 1986, in *Instrumentation in Astronomy VI*, SPIE Conf. 627, 733
- Tucholke H.-J., de Boer K.S., Seitter W.C., 1996, *A&AS* 119, 91
- Vallenari A., Bomans D.J., de Boer K.S., 1993, *A&A* 268, 137
- Weiner B.J., Williams T.B., 1996, *AJ* 111, 1156
- Wilcots E.M., Hodge P.W., King N., 1996, *ApJ* 458, 580
- Will J.-M., 1996, Ph.D. Thesis, University of Bonn
- Will J.-M., Bomans D.J., Vallenari A., Schmidt J.H.K., de Boer K.S., 1996, *A&A* 315, 125